

Design and Energetic Characterization of a Solid-Propellant Self-Powered Robot

Jorge Audrin Morgado de Gois¹

¹ Instituto Militar de Engenharia

Abstract: This paper makes the energetic characterization of a solid-propellant self-powered robot and draws the outlines to design an appropriate dynamical behavior. The proposed approach employs a double-base solid propellant to generate hot gas, which is used to power a pneumatic-type actuation system. In general, such propellant is used in rockets because of its high energy/weight ratio, what makes it very appropriated for extremely power-consuming applications. Traditional designs, one using battery-powered dc motors, another system consisting on a combustion-engine-powered hydraulic actuation and finally, a system based on liquid propellant, are qualitatively analyzed and compared to a solid-propellant design approach. Then, this study shows the energetic modeling, description and analyses of the actuation system of a jumping legged robot, with a cricket-like structure, and a discussion on its dynamical behavior. From the results obtained in simulations, this kind of actuation system seems to be very promising, especially if employed at a multi-degree-of-freedom system. The high average velocity achieved during a very short interval shows the possibility of developing an 'intense' dynamical behavior, with high power and high velocities.

Keywords: solid propellant, mobile robot, actuation potential

NOMENCLATURE

A_p = actuation potential, kJ.kW/kg²
 C = distance from hip joint to attachment of actuator
 e_s = energy density, kJ/kg
 I = impulse
 L = distance from hip joint to MC
 MC = mass center
 P = weight of a body

p_a = maximum power density, kW/kg
 p_s = specific power, kW/kg
 q = independent coordinate
 W = work

Greek Symbols

η = efficiency of conversion and actuation system

Subscripts

G relative to combustion gas
1 relative to rear leg
2 relative to robot body

INTRODUCTION

Everyday, robots are more present in our lives, executing different tasks, in general substituting humans where the task is too dangerous or repetitive, or if a very high precision is necessary. But the growth in their employment is slowed down by a few technological restrictions and, when considering mobile robots, power supply is usually the most serious of such restrictions. The energetic deficiency in current mobile robots does not refer exactly to a small amount of available energy, or even power, but to the relation between available power and the mass of the system. Wheeled robots have a relative good power/mass relation, but they depend on a suitable ground to operate properly, what is not always present (Dunningan, 1996). In such environments, legged robots would represent a good solution, but they suffer of a very poor power/mass relation, what makes impossible to employ them in many of such tasks, which still have to be executed by humans.

Here, it is proposed a new power supply and actuation system based on the use solid propellant, what makes a higher figure of merit possible. This kind of propellant presents a high specific power (Army Science Conference, 2000), what means, it provides an enormous amount of energy from a small mass of propellant in a very short time. This energy is delivered by the gas generator in the form of hot gas – result from the propellant combustion – and can be directly used in a pneumatic system.

In order to use it efficiently the high amount of available power in such a system, the robot has to present a completely new dynamical behavior. Most of legged robots walk in a quasi-static equilibrium, requiring low actuation forces and torques, reducing their energy consumption; on the other hand, these robots have their dynamical performance strongly constrained. A very simple example is the walking pattern of hexapods and quadrupeds: a six-legged robot has a 2-phase walking in order to keep always three standing feet, and a four-legged robot has a 4-phase walking. In such patterns, one group of legs stands while the other one moves, using slow and therefore, power-saving movements. With more power would be possible to these robots to perform a more animal-like walking, that means just like animals do when running, sometimes performing a one-phase walking.

About Power-Source and Actuation System

The main focus in this work relays on the locomotion task of legged robots, which is in general the most power consuming task in mobile robotics. The locomotion system can be divided in two main sub-systems: power source and actuation system. The first concerns to the set of things responsible for energy storage (batteries, fuel and its tank, accumulators, etc...), while the latter represents the devices responsible for transforming the energy into controlled mechanical work (motors, pumps, hydraulic cylinders, etc...).

An important characteristic of the power sources is the energy density e_s – the maximum amount of energy possible to store in the source, divided by its mass. Considering the actuation system, a correspondent characteristic is the maximum power density p_a – maximum amount of power possible to be delivered by the actuation system divided by its mass. There are many possible configurations for power source and actuation system, but some of the most common nowadays are:

- Electrically Actuated: in the case of a battery-powered dc-motor-actuated robot, the energy density of the power source (e_s) is the electrical energy density of the battery. The power density of the energy conversion and actuation system (p_a) is the rated output power of the motor/mechanical converter divided by its mass.
- Hybrid ICE-Hydraulic: in an internal-combustion-engine-powered hydraulically-actuated system, the energy density of the power source is the thermodynamic energy density of the fuel (e.g., gasoline). Finally, the power density of the energy conversion and actuation system would be the maximum output power of the hydraulic actuation system, divided by the combined mass of the engine, pump, accumulator, valves, cylinders, reservoir, and hydraulic fluid of the hydraulic system.
- Liquid Propellant: here, the energy density of the power source is the thermodynamic energy density of the fuel (e.g., hydrazine). The power density of the energy conversion and actuation system is given the maximum output power of the pneumatic actuation system, divided by the sum of its combined mass and the mass of the gas generator.

Based on such characterization it is possible to state a figure of merit, to quantify the energetic performance of the combined power source and actuation system. It is important to emphasize that all these three different configurations present different constructive characteristics, leading to different performances when the whole robot is considered.

Figure of Merit

The Actuation Potential A_p , proposed in Barth et al (2003), is suitable figure of merit to quantify the energetic performance of power supply and actuation system. This performance index is composed by three parameters of primary interest to provide an optimal energetic performance: the energy density, the maximum power density and the efficiency of converting energy from the power source to controlled mechanical work η . Thus, the index can be written as in Eq. (1):

$$A_p = e_s \cdot \eta \cdot p_a \quad (1)$$

The index A_p is justified by the fact that a system with high power-source energy density, high conversion efficiency, and high actuator power density will be the lightest possible system capable of delivering a given amount of power and energy. The index expresses a relation between the power available for execution of a specific task and the overall mass of devices responsible for such execution. In this overall mass are included the masses of power supply, actuators, conductors, converters and any other device involved in supplying energy and transforming it in work for the execution of a task.

But this index may lead to erroneous conclusions too. Let's analyze the case of electrically-actuated human-scale robot: batteries and dc motors (capable of providing the requisite power) offer reasonable conversion efficiency, but provide relatively low power-source energy density and a similarly low actuator/gear-head power density. Now, take as example an ICE-powered hydraulically-actuated large-scale robot, the robot ALDURO (Hiller, German, Morgado, 2004). The use of high power-source energy density (gasoline), in spite of low conversion efficiency and power density of the actuation system, gives a very high actuation potential. Take a third example, the case of a human-scale robot using liquid propellant. Here, the combustion or decomposition of the propellant generates gas with high energy potential, that is, high pressure and temperature. The values for the three examples are shown in Tab. 1.

Table 1 – Comparison of Actuation Potential for different robot configurations

	e_s (kJ/kg)	η	p_a (W/kg)	A_p (kJ.kW/kg ²)
Electric	180	0.55	48	4.8
ALDURO	45000	0.20	44	400
Liquid Propellant	1700	0.09	100	15.3

From the data in Tab. 1, one may wonder that ALDURO has a very high amount of available power to execute the locomotion task; however the truth is not exactly that. If the specific power p_s (the available power divided by the robot mass) is taken, ALDURO presents just 17.8W/kg, while the electric robot has $p_s = 31.6$ W/kg and for liquid propellant system $p_s = 68.8$ W/kg.

It means that, to analyze the dynamical behavior of a robot p_s should be taken, but p_a may be a good indicator for the general energetic performance, affecting many characteristics of the robot as operation time.

The solid propellant system

Since we are searching for is a system able to develop a power demanding dynamics, the specific power seems to be the most important index to consider. That is a very encouraging fact towards the use of pneumatic systems powered by solid propellants, especially when we consider that the energetic density of nitrocellulose is just 1.09MJ/kg, what leads to an actuation potential not so high. It means that as energy source, nitrocellulose is not as good as gasoline because the latter has less energy per unit of mass. At the other side, the burn rate for nitrocellulose is about 10^3 times higher than for an ideal mixture air-gasoline, what makes the nitrocellulose able to deliver a much higher power.

If compared to the hydrazine, nitrocellulose has a lower energy density and a burning rate not much higher. There are two major advantages in using solid instead of liquid propellant: a much simpler implementation is possible, with no valves neither pressure control; the second advantage is the much safer implementation obtained, because the solid propellant is more stable and there is no risk of leakage. The drawback in such implementation consists on the high temperature of the generated gas, which can affect electronic devices of the robot as well as the pneumatic system.

DESIGN OF THE SYSTEM

A very simple system, based on the mechanism of a pistol, will be developed to test the performance of the actuation system and to analyze the dynamical behavior of the robot. It will be a four-legged “jumping robot”, as shown in Fig. 1. Each rear leg have one degree of freedom and is actuated by a pneumatic cylinder, which are modeled as two extra bodies at each leg, linked by translational joints. These joints are provided with springs to help during the take-off and landing phase. When landing, the coils are compressed and locked, absorbing and storing part of the impact energy; during the take off, the springs are released, to improve the jump. The front legs are passive and flexible, just to help the robot to find the correct position at the end of a jump.

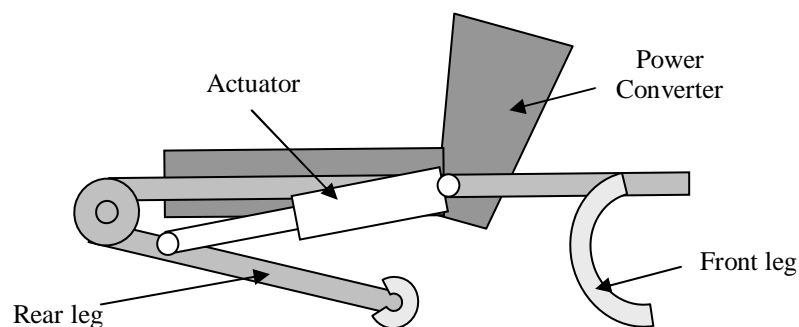


Figure 1 – Schematics of the Solid Propellant Powered Robot

The power converter is composed basically by the pistol body, consisting on a magazine to store the propellant, a loader mechanism and a combustion chamber. There is a distribution valve, which doses the amount of gas to each cylinder (left and right) and an onboard controller to set the distribution valve. The controller is responsible for activating a solenoid, which acts as a trigger to start each jump, which consumes one cartridge of 4.2g. The total capacity of the magazine is 20 cartridges, which are ejected after use. As the pistol body weights 0.95 kg and each actuator weights 0.79 kg, is expected that the robot weights about 4 kg, what means that the mass variation due to cartridge ejection is irrelevant: the robot becomes about 0.1% lighter at the end of a complete run.

Kinematical Model

First, symmetric movement will be considered, that is, the same amount of gas is delivered for both cylinders and planar movement is expected to occur. The movement can be shared in three phases, where the main difference between each one relies on the kinematics topology. They are:

1. *Take-off*: contact occurs just between the robot rear feet and the ground. This phase begins when the propellant is started and lasts up to the loss of contact between rear feet and ground. With a very high friction coefficient between feet and ground, is reasonable to consider no slip; then, contact between rear feet and ground is modeled as a revolute joint.

2. *Flight*: this phase starts at the end of phase 1 and ends when the rear feet meet the ground again. During it, the robot is free in the space.
3. *Landing*: it starts at the end of the flight, with the contact between rear feet and ground. Cinematically it is the same as phase 1.

There is a change in the topology of the system, due to the contact between robot and ground, what is shown in Fig. 2. In phase 1 and 3 the contact is modeled as a single revolute joint, but during phase 2 the robot is free to move in the space, therefore two more degrees of freedom have to be added, what is implemented through the inclusion of two virtual bodies.

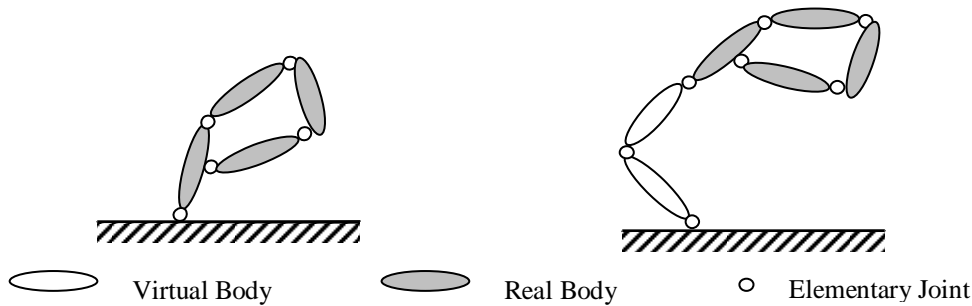


Figure 2 – Kinematical Topology during landing phase (left) and flight phase (right)

The change from one model to another, during the change from phase 1 to 2, is triggered by the vertical component of the constraint force in the revolute joint: when it vanishes the contact is lost. In the same sense, the change from the 4-d.o.f. model to the 2-d.o.f. model is triggered by the position of the rear feet: when it becomes equal to the ground profile height, the model is changed.

Applied Forces

Not only the kinematical topology, but the applied forces change during the robot movement too. Some of these forces are activated by events, while others are not so simple to model or simulate, what leads to a relative complex dynamical model, in spite of a relative simple mechanism. The forces considered as applied to the system are:

- *Weight*: of course, the weights of the bodies act during all the three phases of the movement.
- *Spring Force*: in phase 1, the springs are initially compressed, then are released as soon as the propellant starts to burn (begin of phase 1). They act up to the loss of contact with the ground. During phase 3, they act again to minimize the impact at the landing, acting from the start of contact until they are locked in the rest position of the robot.
- *Front Legs Force*: during the landing (phase 3) the front legs act like springs with high rigidity, activated when their lower point has contact with the ground.
- *Combustion Gases Force*: when combustion of the propellant occurs, begin of phase 1, the generated gas is sent to the pneumatic cylinders (actuators) and the pressure is turned into the actuation force. This force acts up to the cylinder to reach its maximum span, and then the gas is released to atmosphere.

The dynamics of this robot can be described as in Table 2: two different kinematical models and three different sets of applied forces.

Table 2 – Dynamics' Model of the Robot

Phases	Kinematics	Applied Forces
Take-off	2 d.o.f.	1- Weights, Springs, Combustion Gases
Flight	4 d.o.f.	2- Weights
Landing	2 d.o.f.	3- Weights, Spring, Front Leg

A problem arises: what is the function to describe the force exerted by the combustion gases? The modeling of the combustion would lead to a very complicated thermo-dynamical problem, since the burning rate depends on the pressure, which would change in an adiabatic expansion of the gases in the actuator. Another problem to model and simulate such process is the duration of the phenomena: the combustion lasts about 1.6 ms, what would require a very small time step for the simulation of this phase.

To overcome such problem an energetic approach is proposed. Since the used cartridge is standardized, its energetic performance is well known (Bittencourt and Bandeira, 1997): it is able to deliver an amount of energy $W_G = 570$ J and

an impulse $I_G = 2.925$ N.s in the direction of the actuator. Considering that the span of the pneumatic cylinder is long enough to use the whole amount of energy released by the combustion, the work of the combustion gas force is taken as W_G and its impulse as I_G , and the force will not be characterized as a function of time, instead by its work and impulse, what in general is not enough to completely define the problem.

DYNAMICS' MODEL

The combustion gas force acts in phase 1, therefore it is applied to the 2-d.o.f. model, with the set of independent coordinates defined as $\mathbf{q} = [q_1, q_2]$, where: q_1 is the extension of the actuator and q_2 represents the angle between the rear leg and the ground. If $\boldsymbol{\beta}$ is a set of dependent coordinates, which completely determines the robot configuration, a set of constraint equations $\mathbf{g}(\boldsymbol{\beta}, \mathbf{q}) = \mathbf{0}$ can be stated to describe the relation between dependent and independent coordinates.

The kinematical loop composed of rear leg, body and actuator has an explicit solution for $\boldsymbol{\beta}$ as function of \mathbf{q} , what enables to write $\boldsymbol{\beta} = \mathbf{g}^*(\mathbf{q})$. From this relation is very easy to state the relation between the velocities, as stated in Eq. 2.

$$\dot{\boldsymbol{\beta}} = \frac{\partial \mathbf{g}^*}{\partial \mathbf{q}} \dot{\mathbf{q}} = J_q(\mathbf{q}) \cdot \dot{\mathbf{q}} \quad (2)$$

In Eq. 2, J_q represents the Jacobean matrix of the set of kinematical constraints with respect to the independent coordinates. If the set $\boldsymbol{\beta}$ is composed of centroidal coordinates, the kinetic energy E of the system may be written as function of the independent velocities in Eq. 3.

$$E(\mathbf{q}, \dot{\mathbf{q}}) = \frac{1}{2} \cdot \dot{\boldsymbol{\beta}}^T \cdot M \cdot \dot{\boldsymbol{\beta}} = \frac{1}{2} \cdot J_q^T \cdot \dot{\mathbf{q}}^T \cdot M \cdot J_q \cdot \dot{\mathbf{q}} \quad (3)$$

Considering the work of all applied forces in phase 1, that is, work of weights $W_w(q_1, q_2)$, work of combustion gas force W_G and the work of the spring force $W_s(q_1, q_2)$, using Eq. 3 we can make an energy balance in Eq. 4.

$$E(\mathbf{q}, \dot{\mathbf{q}}) = W_G + W_w(\mathbf{q}) + W_s(\mathbf{q}) \quad (4)$$

In the same fashion, the impulse may be expressed in terms of \mathbf{q} , by taking the variation of momentum (Greenwood, 1977). If the piston and the cylinder of the actuator are taken as the third and fourth bodies, the generalized impulse \mathbf{I} given by Eq. 5, which accounts for impulse due to the gas force I_G and to the impulse I_s of forces exerted by the springs of constant k . If the initial conditions are null, Eq. 6 holds.

$$\mathbf{I} = [0_{\text{bx6}} \quad ; \quad I_G + 2I_s \quad ; \quad 0_{\text{bx2}} \quad ; \quad -I_G - 2I_s \quad ; \quad 0_{\text{bx2}}]^T \quad (5)$$

$$J_q^T \cdot M \cdot J_q \cdot \dot{\mathbf{q}} = J_q^T \cdot \mathbf{I} \quad (6)$$

Now, from Eq. 4, 5 and 6, we have three scalar equations but four unknowns ($q_1, q_2, \dot{q}_1, \dot{q}_2$), thus one more equation is necessary. Such equation comes from the robot operation: the gas force acts until the actuator piston reaches its maximum stroke q_{1max} , then the gas is released to the atmosphere and there is no more gas force. Hence, at the end of the actuation force Eq. 7 gives the extension of the actuator.

$$\text{Gas Force} = 0 \rightarrow q_{1max} = q_1 \quad (7)$$

From Eqs. 3, 4, 6 and 7, it is possible to state the configuration of the robot at the end of the actuation of the combustion gas, what is not necessarily the end of phase 1.

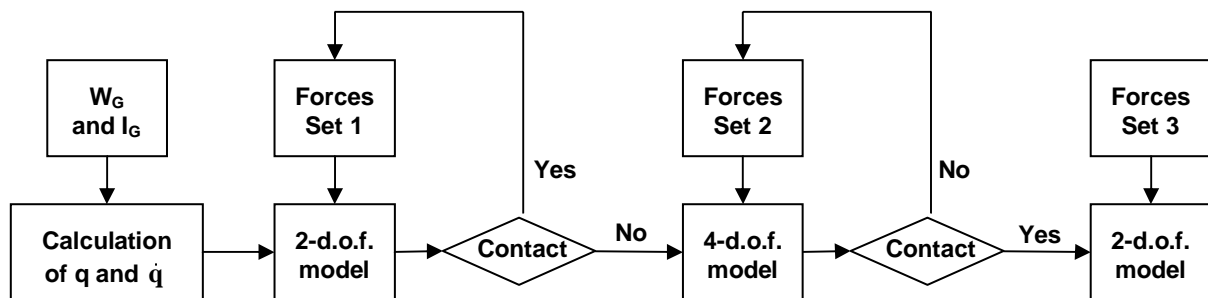


Figure 3 – Sequence of used models

As the real interest here in this paper is the locomotion capacity of the robot, it is not necessary to simulate the actuation process; we can use the known configuration at the end of the actuation as initial condition to proceed a multi-body simulation from this point on.

The whole process of changing models is pictured in Fig. 3. As already explained, the transition from phase 1 to phase 2 occurs at the vanishing of the constraint force in the revolute joint on the rear feet; simultaneously, the 2-d.o.f. model is replaced by the 4-d.o.f. model, using the last configuration of phase 1 as initial condition for phase 2. Later, the change from phase 2 to 3 will be triggered by the contact between rear feet and ground, and the 2-d.o.f. model will be employed again to run a multi-body simulation until the robot reaches its equilibrium position..

SIMULATIONS AND RESULTS

Using the composition of models shown in Fig. 3, some simulations are run for the estimation of parameters. Through the solution of the system stated by 4, 6 and 7, the configuration of the robot at the end of the actuation of the combustion gas force is obtained. In Fig. 4 two plots are shown: of the horizontal and the vertical velocities of the robot’s mass center (MC) at the end of the actuation.

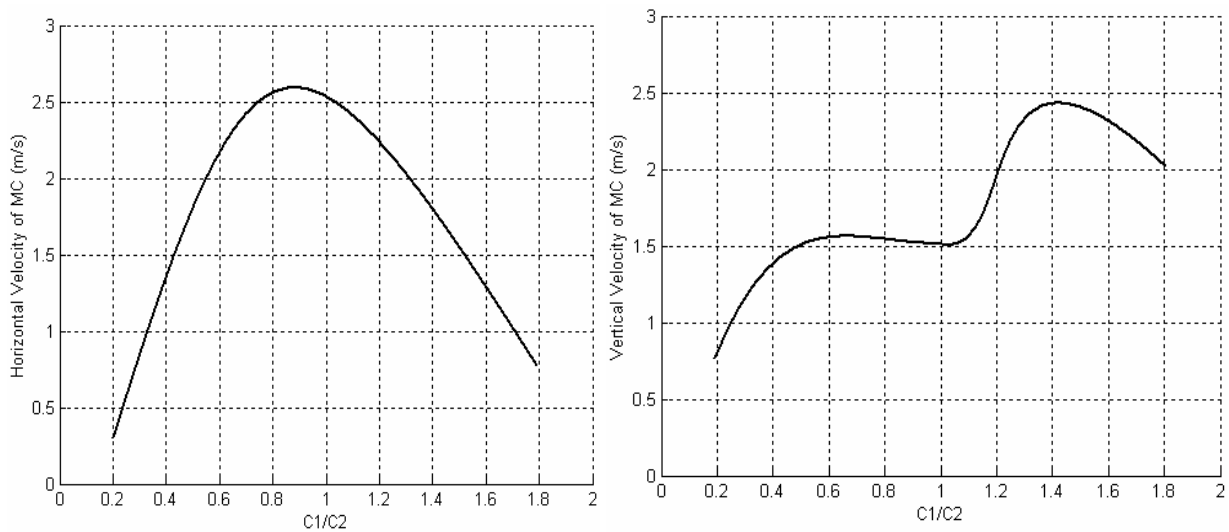


Figure 4 – Horizontal (left) and Vertical (right) Velocities of robot MC at the end of gas action versus C_1/C_2

The plots in Fig. 4 show the variation in the velocity of robot’s mass center according to the ratio C_1/C_2 , where the numerator is the distance from the actuator attachment point on the robot body to the hip joint, and the denominator corresponds to the distance between the hip joint and the attachment point on the rear leg.

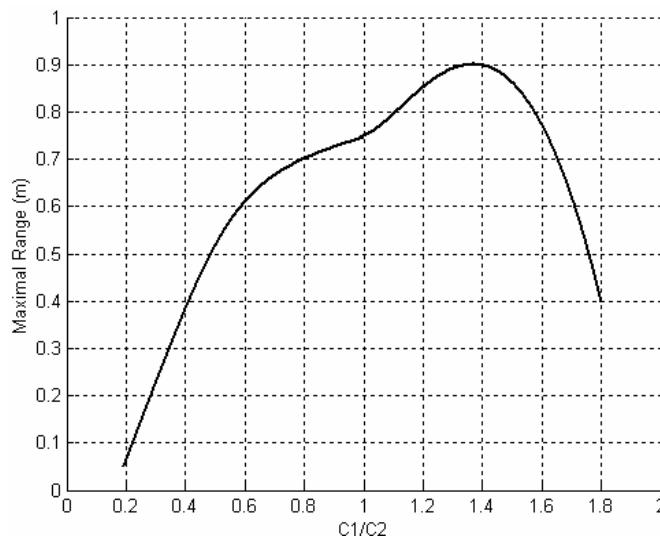


Figure 5 – Maximum range for different C_1/C_2

With help of the energy (Eq. 4) and momentum (Eq. 6) equations, the configuration of the robot at the end of actuation is obtained. This configuration is used as initial condition to run a simulation using the multi-body model of the take-off phase. Then, the simulation follows as shown in Fig.3, and results for maximal range are shown in Fig. 5. In this figure, it is clear that the relative orientation of the actuator has a strong influence on the range.

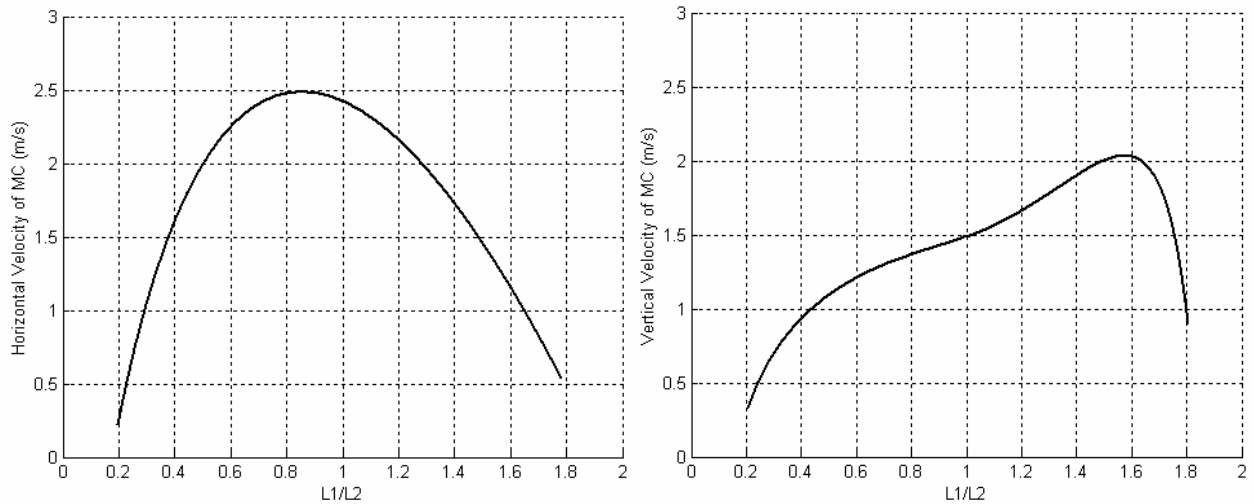


Figure 6 – Horizontal (left) and Vertical (right) Velocities of robot MC at the end of gas action versus L_1/L_2

New simulations are run, now keeping the ratio C_1/C_2 constant and equal to 1, and varying the ratio L_1/L_2 , where the numerator represents the length of the rear leg and the denominator is the double of the distance between the mass center of the robot body and the hip joint.

From Fig. 6 it is easy to see that this second ratio has a strong influence on final velocities achieved at the end of actuation. The ranges obtained from the velocities presented in Fig. 6 are shown in Fig. 7.

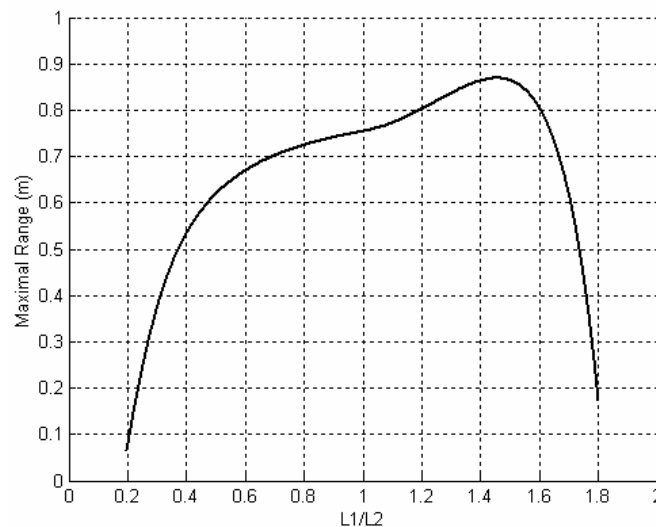


Figure 7 – Maximum range for different C_1/C_2

CONCLUSIONS

Two points are important to highlight:

- The maximal range achieved by variation of the geometric configuration of the robot is 0.93m for one shot. The robot may carry 20 cartridges, what leads to a total possible range of 18.6m.
- Each jump took a time interval of 0.21s, what represents an average horizontal velocity of 4.42m/s.

Considering the size and mass of the robot, and that we are talking about a legged robot, the results show that such kind of system is very promising. The high average velocity achieved during a very short interval shows the possibility of developing an 'intense' dynamical behavior, with high power and high velocities. Further studies will concern to the use of a continuous gas generation, what will enable autonomy enough to carry on real operations.

REFERENCES

- Army Science Conference. "Accelerating the pace of transformation to the objective force". Baltimore, 2000. 1 CD-ROM.
- Barth, E.J., Gogola, M.A, Goldfarb, M. "Modeling and Control of a Monopropellant-Based Pneumatic Actuation System". Proceedings of the 1003 IEEE International Conference 00 Robotics &Automation Taipei, Taiwan, September 14-19,2003
- Bittencourt, G.A.; Bandeira, E.L.; "Mapeamento da Velocidade de Boca de uma Munição 9mm Utilizando Lógica Fuzzy". Instituto Militar de Engenharia. IME. Rio de Janeiro, RJ – BR. Novembro de 2001.
- Dunningan, James F. "Digital Soldiers: the evolution of high-tech weaponry and tomorrow's brave new battlefield". USA, october 1996.
- Greenwood, D.T. "Classical Dynamics". Dover Publications. NY – USA. 1977.
- Hiller, M.; Germann, D.; Morgado de Gois, J. A.; Design and control of a quadruped robot walking in unstructured terrain. IEEE Conference on Control Applications, CCA 2004, Taipei, Taiwan, 2004.

RESPONSIBILITY NOTICE

The author is the only responsible for the printed material included in this paper.